Article

Discovery Medicine 2025; 37(197): 1082–1095
https://doi.org/10.24976/Discov.Med.202537197.96

Combined Oral Contraceptives Modulate Apoptosis via IL-11/PI3K/AKT Pathway in Rat With Premature Ovarian Insufficiency

Meiling Chen[1], Fan Zhang[2], Fang You[2], Li Zhang[2], Li Zeng[2,*]

[1]Second Clinical Medical College, Guizhou University of Traditional Chinese Medicine, 550025 Guiyang, Guizhou, China
[2]Department of Gynecology, The Second Affiliated Hospital of Guizhou University of Traditional Chinese Medicine, 550001 Guiyang, Guizhou, China
*Correspondence: zengli261@gzy.edu.cn (Li Zeng)
Published: 9 June 2025

Background: Premature ovarian insufficiency (POI) is characterized by a reduction in primary follicle count along with abnormal follicle development. This study aims to explore the impact of combined oral contraceptives (COCs) on the apoptosis of ovarian granulosa cells, which are instrumental for follicular development, in POI and the underlying mechanisms, to provide theoretical guidance for the treatment of POI.

Methods: A rat model of POI was established using tripterygium glycoside tablets. After treatment with COCs, the therapeutic effect of the animals was verified by means of hematoxylin-eosin staining, immunohistochemistry, and enzyme-linked immunosorbent assay (ELISA). Flow cytometry, cell counting kit-8 (CCK-8), quantitative polymerase chain reaction, and Western blotting were utilized to investigate the impact of COCs on granulosa cell apoptosis, as well as the function of the interleukin (IL)-11/phosphoinositide 3-kinase (PI3K)/protein kinase B (AKT) signaling pathway. Further experiments were also conducted to verify whether COCs could inhibit granulosa cell apoptosis through this pathway.

Results: COCs treatment was effective in improving ovarian granulosa cell status, reducing luteinizing hormone (LH) and follicle-stimulating hormone (FSH) levels, and increasing estradiol levels in the POI rats ($p < 0.01$). IL-11 silencing promoted apoptosis in POI granulosa cells by inhibiting the PI3K/AKT pathway. COCs treatment partially reversed these effects by upregulating IL-11 expression and restoring PI3K/AKT pathway activity. This resulted in increased levels of B-cell lymphoma 2 (*Bcl-2*) ($p < 0.05$) and cytochrome P450 family 19 subfamily A member 1 (*CYP19A1*) ($p < 0.01$), while suppressing the expression of Bax and cleaved-cysteine-aspartic acid protease 3 (cleaved-caspase 3) ($p < 0.001$).

Conclusion: Our findings demonstrated that COCs protect ovarian granulosa cells from apoptosis in rats with POI, an effect mediated through the IL-11/PI3K/AKT signaling cascade.

Keywords: POI; COCs; ovarian granulosa cells; IL-11/PI3K/AKT; apoptosis

Introduction

The pathogenesis of premature ovarian insufficiency (POI), a condition substantially affecting female reproductive health, is multifaceted, involving aspects such as genetics, immunity, environment, and hormones [1]. POI typically manifests prior to the age of 40, leading to a decline in female reproductive capacity, abnormal sex hormone levels, and a range of additional adverse symptoms [2]. As a key component of ovarian structure and function, the health status of follicular granulosa cells is directly related to the development of follicles, the maturation of oocytes, and the synthesis and secretion of ovarian hormones [3]. It is known that follicular atresia, attributed to abnormal apoptosis of ovarian granulosa cells, is the primary condition contributing to the development of POI [4]. Therefore, in-depth exploration of the regulatory mechanism of follicular granulosa cell apoptosis is of great significance for unraveling the pathogenesis of POI and developing effective therapeutic strategies.

Apoptosis, a type of genetically regulated programmed cell death, is essential for the development of multicellular organisms, playing a role in maintaining tissue homeostasis and the regulation of disease progression [5]. B-cell lymphoma 2 (Bcl-2) can delay cell apoptosis, while Bcl-2-associated X protein (Bax), an inhibitor of Bcl-2, promotes cell apoptosis [6]. Related studies have shown that Bax and Bcl-2 expression produce important regulatory effects on ovarian granulosa cell apoptosis [7,8]. Regardless of the regulatory mode for apoptosis, caspase 3 in the caspase pathway is the major player in the apoptosis process [9]. Interleukin (IL)-11 is a multifunctional cytokine with a variety of biological processes that promote cell proliferation, inhibit apoptosis, participate in inflammatory responses, and modulate immune responses [10,11]. In the reproductive system, IL-11 has been shown to in-

fluence processes such as follicular development, oocyte maturation, as well as luteinization [12,13]. Therefore, its abnormal expression may be closely related to the onset of POI. The phosphoinositide 3-kinase (PI3K)/protein kinase B (AKT) signaling pathway represents a vital cellular signaling mechanism, implicated in diverse biological processes encompassing cell growth, differentiation, and programmed cell death [14]. In the reproductive system, the PI3K/AKT pathway represents a vital cellular signaling mechanism, implicated in diverse biological processes such as cell growth, differentiation, and programmed cell death [15]. Studies have indicated that IL-11 impacts the PI3K/AKT signaling pathway, significantly influencing bone metabolic balance, adipocyte expansion, and oncogenic cell invasion and dissemination [16–18]. However, studies focusing on dissecting whether IL-11 can act on POI through the PI3K/AKT pathway remain relatively scarce.

Combined oral contraceptives (COCs) represent a class of artificially synthesized estrogen-progestin complexes with high activity. This class of contraceptives has been found to decrease concentrations of follicle-stimulating hormone and luteinizing hormone in individuals with POI, while preventing premature follicle recruitment and promoting follicle development synchronization [19,20]. Therefore, COCs may be associated with ovarian granulosa cell apoptosis in POI. Owing to usage convenience and low cost, COCs are widely employed in the treatment of premature ovarian dysfunction in patients with POI, although their mechanism of action and effectiveness need to be further explored.

The objective of this study is to investigate the therapeutic effects of COCs (desogestrel tablets) in POI. Animal and cell experiments were conducted to explore whether COCs can alleviate symptoms of POI rats through the IL-11/PI3K/AKT pathway. This research not only significantly broadens our understanding of the pathogenesis of POI but also provides a novel perspective and strategy for expanding POI treatment options.

Materials and Methods

Construction and Sampling of the POI Rat Model

Fourteen specific pathogen-free (SPF)-grade Sprague–Dawley rats (female, each weighing 250 ± 20 g, aged 3 months) were acquired from Chongqing Ensiweier Biotechnology Co., Ltd. (Chongqing, China). The animals were acclimatized for one week in an animal facility with a temperature of 23 ± 2 °C, a humidity of 35–60%, and a day-night alternation of 12–12 h. During the period of feeding, vaginal shedding of cells was observed. A week later, the female rats with normal estrous phase were selected for modeling. Tripterygium glycosides tablet (20230102, Yuanda Pharmaceutical Huangshi Feiyun Pharmaceutical Co., Ltd., Huangshi, China) at the daily dose of 80 mg/kg was intragastrically administered to each animal, and vaginal shedding cell smears were prepared starting day 8 to monitor changes in the estrous cycle. The disease modeling is considered successful when the vaginal cell smears from rats with estrous disorders have become almost uninterpretable, undermining researchers' ability to evaluate their estrus cycle (preestrous, estrous, postestrous and interestrous) [21].

The successfully modeled rats were then randomly assigned to two groups: the Model group and the Model + COCs group. Based on the therapeutic cycle of combined oral contraceptives (COCs) in humans and the dose conversion between humans and animals [22,23], rats in the Model + COCs group were administered a solution containing 0.002% deoxynorethindrone estradiol (H20130491, N.V. Organon, Oss, Netherlands). The solution was administered intragastrically at 10 mL/(kg·d) for a continuous period of 21 days. The Model group received an equivalent volume of distilled water. After completion of the administration, the rats were rendered unconscious via intraperitoneal administration of a 3% pentobarbital sodium (P3761, Beijing Zongheng Science Co., Beijing, China) at 40 mg/kg. Serum samples were obtained from the animals. Euthanasia was performed by injecting ≥150 mg/kg of pentobarbital sodium into the tail vein of each animal. Post-injection, the death of these rats was confirmed through cessation of breathing, absence of heartbeat, and loss of corneal reflex. Finally, the rats were dissected to extract their ovarian tissues.

Hematoxylin-Eosin Staining

The ovarian tissues were prepared into paraffin slices, dewaxed, rehydrated, and then stained with hematoxylin dye (G1004, Servicebio, Wuhan, China) and eosin dye (G1002, Servicebio, Wuhan, China). Subsequently, the slices underwent dehydration and were then embedded in neutral resin (10004160, Sinopharm, Beijing, China) prior to observation using a microscope (MF53, Mshot, Guangzhou, China).

Immunohistochemical Detection

The ovarian tissue was washed with phosphate-buffered saline (PBS) and fixed with 4% paraformaldehyde. Subsequently, after gradient ethanol dehydration, xylene transparency, and paraffin embedding, the sections were obtained. Then the sections were dewaxed, rehydrated, and subjected to antigen retrieval. Goat serum (C0265, Beyotime, Shanghai, China) was employed for blocking of nonspecific sites, and then the samples were subjected to incubation with primary antibody (1:200), followed by secondary antibody (1:50) treatment. After 3,3'-diaminobenzidine (DAB) development (ZLI-9019, ZSGB-BIO, Beijing, China), hematoxylin was used to dye the nuclei. Finally, the sections were dehydrated and sealed with a neutral resin (10004160, Sinopharm, Beijing, China) and then observed using an Mshot MF53 microscope (Guangzhou Micro-shot Technology Co., Ltd., Guangzhou,

China). The immunofluorescence images were imported into Image pro plus 6.0 (Media Cybernetics, Media Cybernetics, Rockville, MD, USA), in which the threshold was set to distinguish the positive area from the background, the area and integrated optical density (IOD) were measured, and the average optical density (AOD) was calculated using the formula below:

$$\text{AOD} = \text{Mean IOD/Mean area.}$$

Primary antibodies used in this experiment include anti-AKT1 (A17909, ABclonal, Wuhan, China), anti-cleaved-caspase 3 (bsm-61090R, Bioss, Beijing, China), and anti-PI3 kinase p110 delta (A19742, ABclonal, Wuhan, China). Horseradish peroxidase (HRP)-labeled goat anti-rabbit immunoglobulin G (IgG) (H + L) (A0208, Beyotime, Shanghai, China) was used as the secondary antibody.

Enzyme-Linked Immunosorbent Assay (ELISA) Detection

Rat serum was obtained by retrieving the supernatant following the centrifugation (at 2000 rpm for 20 min) of the blood specimen prewarmed at room temperature for 10–20 min. The cell was diluted with phosphate-buffered saline (PBS; G002, Servicebio, Wuhan, China). Cells from each group were collected, and 500 µL of lysis buffer (E051, Fine Test, Wuhan, China), along with 5 µL of phenylmethylsulfonyl fluoride (PMSF) (E051, Fine Test, Wuhan, China), was added. The cell suspension was left to stand on ice for 30 min prior to centrifugation to obtain supernatant.

The expression levels of luteinizing hormone (LH; CB10446-Ra, Coibo bio, Shanghai, China), rat follicle-stimulating hormone (FSH; CB10273-Ra, Coibo bio, Shanghai, China), rat testosterone (CB10386-Ra, Coibo bio, Shanghai, China), and estradiol (CB10266-Ra, Coibo bio, Shanghai, China) in rat serum were determined using the ELISA kit customized for rat sample uses. Estradiol was detected in cells using Rat E2 (Estradiol) ELISA Kit (ER1507, Fine Test, Wuhan, China). Specific operations are as follows: The ELISA assay involves setting up blank, standard, and sample wells on an enzyme-labeled plate. Standards of varying concentrations were added to standard wells (50 µL per well), while 40 µL diluent plus 10 µL sample (serum or cell suspension) was added to each sample well. Enzyme-labeled reagent (100 µL) was added to every well except the blank wells. After sealing and incubating at 37 °C for 1 h, the plates were washed 5 times, followed by the addition of chromogenic reagents A+B (50 µL per well) and incubation in the dark for 15 min. The reaction was terminated by the addition of stop solution, and absorbance was measured at 450 nm using a microplate reader (NanoDrop One/One C, Thermo Fisher Scientific, Waltham, MA, USA). LH, FSH, testosterone and estradiol levels were calculated from standard curves plotted with known concentrations of the standards used.

Isolation and Culture of Granulosa Cells From Ovaries of POI Rats

One milliliter of trypsin was added to the dissected ovarian tissue and incubated in a water bath set at 37 °C for 10 min. The digestion was repeated 5–6 times until the trypsin solution became clear; subsequently, 2 mL of complete medium was supplemented to terminate digestion. The mixture was then subjected to centrifugation (2500 rpm, 3 min) and the supernatant was discarded. The pellet was then resuspended with complete medium prior to another round of centrifugation. After discarding the supernatant, the pellet was resuspended in complete medium again. The cell suspension (2×10^5 cells/well) was inoculated and cultured in a culture dish for 24 h. Finally, the cells were observed under a microscope. The cultured granulosa cells were regularly tested for mycoplasma contamination using quantitative polymerase chain reaction (qPCR)-based methods, and the results were negative.

Identification of Ovarian Granulosa Cells

Rat cardiomyocytes H9c2 (2-1) (CL-0089, Procell, Wuhan, China) were used as the negative control. The cells were subjected to STR identification and mycoplasma detection by the manufacturer, and the result of the mycoplasma detection was negative. Both H9c2 (2-1) and granulosa cells (1×10^6 each) were resuspended in 100 µL of PBS. Subsequently, 5 µL of anti-anti-follicle-stimulating hormone receptor (FSHR) polyclonal antibody (22665-1-AP, Thermo Fisher Scientific) was added, and the mixture was incubated at room temperature in the dark for 20 min. After centrifugation at 1000 rpm for 5 min, the supernatant was discarded. The cells were then washed with 1 mL of PBS, centrifuged again, and the supernatant was removed. The cell pellet was resuspended in 100 µL of PBS, and 5 µL of goat anti-rabbit IgG (H+L) secondary antibody labeled with Fluorescein isothiocyanate (FITC) (F-2765, Thermo Fisher Scientific) was added. The cells were incubated at room temperature in the dark for 20 min, followed by centrifugation and removal of the supernatant. The cells were washed with 1 mL of PBS and centrifuged to discard the supernatant. Finally, the cells were resuspended in 200 µL of PBS and analyzed by CytoFLEX flow cytometry (Beckman Coulter, Brea, CA, USA).

Flow Cytometry

Following the instructions of the Annexin V FITC/Propidium Iodide (PI) Apoptosis Detection Kit (40302ES50, Yeasen, Shanghai, China), the cells were washed with pre-cooled PBS twice, then the PBS was discarded, and the cells were resuspended in 100 µL of 1× binding buffer. Annexin V-FITC (5 µL) and PI dye (10 µL) were subsequently added. The reaction was carried out at room temperature for 10–15 min and then 400 µL of 1× binding buffer was added to the reactants. Apoptosis

was detected by means of flow cytometry (BeamCyte, Antpedia, Changzhou, China) within 1 h. The total apoptosis rate was determined as follows:

$$\text{Total apoptosis rate} = \text{Late apoptosis rate} + \text{Early apoptosis rate}.$$

Cell Counting Kit-8 (CCK-8) Detection

Primary ovarian granulosa cells of POI rats were inoculated in 96-well plates (5000 cells per well), and COCs were dissolved with dimethyl sulfoxide (DMSO) and added to the medium for 24 h. Each well received 10 µL of CCK-8 solution (C0038, Beyotime, Shanghai, China) and was then incubated for 1 h in a cell culture incubator. Subsequently, the absorbance at 450 nm was assayed using an ELISA reader (cMAXPlus, MOLECULARDEVICES, Sunnyvale, CA, USA). The cell viability percentage and cell inhibition rate were determined using the formulas below:

$$\text{Cell viability (\%)} = (\text{OD}_{\text{sample}} - \text{OD}_{\text{blank}})/(\text{OD}_{\text{control}} - \text{OD}_{\text{blank}}) \times 100;$$

$$\text{Cell inhibition rate (\%)} = 1 - \text{viability}.$$

The data obtained were imported into GraphPad Prism 8 (GraphPad Software Inc., San Diego, CA, USA). The "log(inhibitor) vs. response-variable slope" curve fitting method was employed to calculate the half-maximal inhibitory concentration (IC50) of the COCs.

qPCR

Primary ovarian granulosa cells were isolated from POI rats and were subjected to COCs treatment or plasmid transfection according to the experimental groups. Afterwards, RNA was extracted by isopropanol precipitation [24], and first-strand cDNA was synthesized using Golddenstar™ RT6 cDNA Synthesis Kit Ver.2 (TSK30, QingKe, Beijing, China). Each component was mixed with 2× T5 Fast qPCR Mix (SYBR Green I) (TSE20, QingKe, Beijing, China), and then the qPCR reaction was performed on Bio-Rad iQ™ 5 (Bio-Rad, Hercules, CA, USA). Glyceraldehyde-3-phosphate dehydrogenase (GAPDH) served as the internal control, and relative gene expression was calculated using the $2^{-\Delta\Delta Ct}$ method. The primers utilized for testing are listed in Table 1.

Table 1. Primer sequences.

Primer	Sequence (5′ – 3′)
IL-11-F	GCTTCCTGGAGTGCTGACAA
IL-11-R	GTAAGCGACGAAGTAGCCGT
PI3K-F	ACCTGTGCCTTCTGCCTTAC
PI3K-R	ATCTTTGAATGCCCCCGTGT
AKT-F	GATGGACTCAAACGGCAGGA
AKT-R	AGCACCTGAGTTGTCACTGG
Bcl-2-F	GAACTGGGGGAGGATTGTGG
Bcl-2-R	GGGGTGACATCTCCCTGTTG
Bax-F	CGTCTGCGGGGAGTCACG
Bax-R	AGCCATCCTCTCTGCTCGAT
Caspase 3-F	ACCGATGTCGATGCAGCTAA
Caspase 3-R	GGTGCGGTAGAGTAAGCATA
CYP19A1-F	TGACGTCACTGACAACTCGG
CYP19A1-R	CCCCAGGAAGAGCGTGTTAG
GAPDH-F	CAATCCTGGGCGGTACAACT
GAPDH-R	TACGGCCAAATCCGTTCACA

IL-11, interleukin-11; *PI3K*, phosphoinositide 3-kinase; *AKT*, protein kinase B; *Bcl-2*, B-cell lymphoma 2; *Bax*, Bcl-2-associated x protein; *Caspase 3*, cysteine-aspartic acid protease 3; *CYP19A1*, cytochrome P450 family 19 subfamily A member 1; *GAPDH*, glyceraldehyde-3-phosphate dehydrogenase; F, forward; R, reverse.

Western Blotting

The cells were transferred into 1.5 mL tubes and centrifuged at 3000 rpm for 5 min. The pellet was washed with PBS, followed by centrifugation again. Radioimmunoprecipitation assay lysis buffer (RIPA) lysis buffer (P0013B, Beyotime, Shanghai, China) was added, followed by incubation on ice for 10 min. Finally, the samples were centrifuged at 13,000 rpm for 20 min at 4 °C, and the supernatant was collected as the total protein sample. Total protein at 500 µg was mixed with 5× SDS loading buffer (8015011, Dakewei, Beijing, China) at a 4:1 ratio. The protein was denatured by heating in a metal bath, and 60 µg samples were applied to SDS-PAGE for electrophoresis, followed by membrane transfer. After blocking was performed, primary antibody (1:1000) and secondary antibody (1:2000) incubation were sequentially conducted, prior to color development. Finally, the blots were visualized utilizing a gel imaging system (34580, Thermo Fisher Scientific) and finally developed using a nucleic acid protein gel imager (Universal Hood II, Bio-Rad, Hercules, CA, USA). In Image Lab (Bio-Rad) software (Bio-Rad, Hercules, CA, USA), the grayscale value of each band was determined. The relative expression level of a target protein was measured by dividing its gray value by the gray value of GAPDH. The gray value of the control group was set as 1, which was standardized for the other experimental groups.

Primary antibodies used in this experiment include anti-IL-11 (A1902, Abclonal, Wuhan, China), anti-PI3K (A0265, Abclonal, Wuhan, China), anti-phosphorylated phosphoinositide 3-kinase (p-PI3K) (AP0427, Abclonal, Wuhan, China), anti-AKT (9272, Cell Signaling Technology, Danvers, MA, USA), anti-phosphorylated protein kinase B (p-AKT) (4060, Cell Signaling Technology), anti-Bcl-2 (A19693, Abclonal, Wuhan, China), anti-Bax (A19684, Abclonal, Wuhan, China), anti-cleaved-caspase 3 (AF7022, Affinity Biosciences Ltd., Melbourne, Aus-

tralia), anti-CYP19A1 (A1373, Abclonal, Wuhan, China), anti-GAPDH (A19056, Abclonal, Wuhan, China). HRP-conjugated Goat anti-Rabbit IgG (H+L) (AS014, Abclonal, Wuhan, China) was utilized as the secondary antibody.

Plasmid Transfection

Coded fragments based on IL-11 were constructed on the pLVX-IRES-puro vector (VT1464, YouBio, Changsha, China) to obtain oe-IL-11 plasmids, and sh-IL-11 was constructed with pLVX-shRNA1 (VT1456, YouBio, Changsha, China) as a vector. Before transfection, the ovarian granulosa cells of POI rats were spread in 10 cm culture dishes at a rate of 5×10^6 per dish. Fresh culture medium was replaced 24 hours later.

10 µg of each plasmid (oe-NC, oe-IL-11, sh-NC, and sh-IL-11) was individually dissolved in 490 µL of Opti-MEM | Reduced Serum Medium (OPTI-MEM) (31985070, Gibco, Waltham, MA, USA), while 30 µL of the transfection reagent Max (24765-1, BioMedicine, Chongqing, China) was diluted in 470 µL of OPTI-MEM. Both solutions were mixed thoroughly and incubated for 5 min at room temperature. Subsequently, the transfection reagent mixture was gently combined with the plasmid-containing solutions, followed by a 15-minute incubation. The resulting mixtures were then evenly distributed into culture dishes. After continuous incubation of the cells for 48 h, stable cell lines expressing oe-NC, oe-IL-11, sh-NC, and sh-IL-11 were established. The sequences of the interference target, empty vector, oe-IL-11, and sh-IL-11 insertion are provided in the **supplementary information**.

Data Analyses

Statistical analyses were conducted using GraphPad Prism 8. Data are expressed as mean ± standard deviation (SD). The Shapiro–Wilk test was used to assess the normal distribution of data. For data that conform to a normal distribution, a *t*-test was used to detect differences between two groups. For comparisons among multiple groups, variance homogeneity was assessed using Levene's test. If variance homogeneity was satisfied, one-way analysis of variance (ANOVA) with Tukey's post-hoc test was applied.

Results

Effect of COCs on POI Rats

To explore the therapeutic effect of COCs on POI rats, HE staining was first performed on the ovarian tissues of the Model group and the Model + COCs group. It was found that some follicles in the Model group had only follicular cavities, along with several blocked follicles. The granulosa cells in the Model group appeared in a disorderly arrangement. In the Model + COCs group, the ovarian architecture remains intact, devoid of atretic follicles, with the granulosa cells arranged neatly (Fig. 1A). Immunohistochemical analysis revealed that the Model + COCs group exhibited notably elevated expression levels of PI3K ($p < 0.05$) and AKT ($p < 0.01$) proteins, compared to the Model group, while demonstrating a marked decrease in the expression of cleaved-caspase 3 protein ($p < 0.05$) (Fig. 1B–E). In addition, serum concentrations of LH, FSH, testosterone, and estradiol in rats were assayed via ELISA. The outcomes indicated that, in comparison to the Model group, the Model + COCs group displayed significantly decreased serum levels of LH and FSH, whereas the levels of testosterone and estradiol were notably elevated ($p < 0.01$) (Fig. 1F–I). These results suggested that COCs might alleviate ovarian disorders in POI rats by improving the integrity of ovarian tissue structure, regulating hormone levels, and acting on apoptosis-related pathways.

Morphological Observation and Identification of POI Rat Ovarian Granulosa Cells

The isolated POI rat ovarian granulosa cells were cultured for 24 h, and then they were observed under a microscope. The cells were found to exhibit adherent growth (Fig. 2A). FSHR is a distinctive membrane protein of ovarian granulosa cells and can be used for their identification, employing flow cytometry to detect its expression in the cells. The results showed that the positive percentage was greater than 85%, indicating their suitability for subsequent experiments (Fig. 2B,C).

Effect of COCs on Apoptosis in Primary Ovarian Granulosa Cells of POI Rats

To further explore the effect of COCs on the apoptosis of ovarian granulosa cells of POI rats, primary cells from these rats were exposed to varying concentrations of COCs, and the IC50 of COCs on the cells was determined (Fig. 3A). Therefore, the cells in the Model + COCs group were treated with 122 ng/mL of COCs. The experimental outcomes indicated that, in comparison to the control group, the Model group exhibited a significant elevation in cell apoptosis rate, accompanied by a decrease in cell viability and a notable reduction in estradiol expression level ($p < 0.001$). However, compared to the Model group, the apoptosis rate of cells in the Model + COCs group was significantly lower ($p < 0.001$), with a marked improvement in cell viability and a notable increase in estradiol levels ($p < 0.01$) (Fig. 3B–E). *CYP19A1* is responsible for converting androgens into estrogens [25], and its expression is consistent with that of estradiol. In addition, the Model group demonstrated a marked reduction in *IL-11* and *Bcl-2* gene and protein expression, accompanied by a significant elevation in *Bax* expression, when compared to the control group ($p < 0.001$). Conversely, the POI + COCs group exhibited an inverse pattern of expression for these genes and proteins relative to the Model group. At the same time, the Model + COCs group exhibited a marked elevation in the ratio of p-PI3K to PI3K, as well as p-AKT to AKT, when compared to the Model group ($p < 0.001$). The POI + COCs group

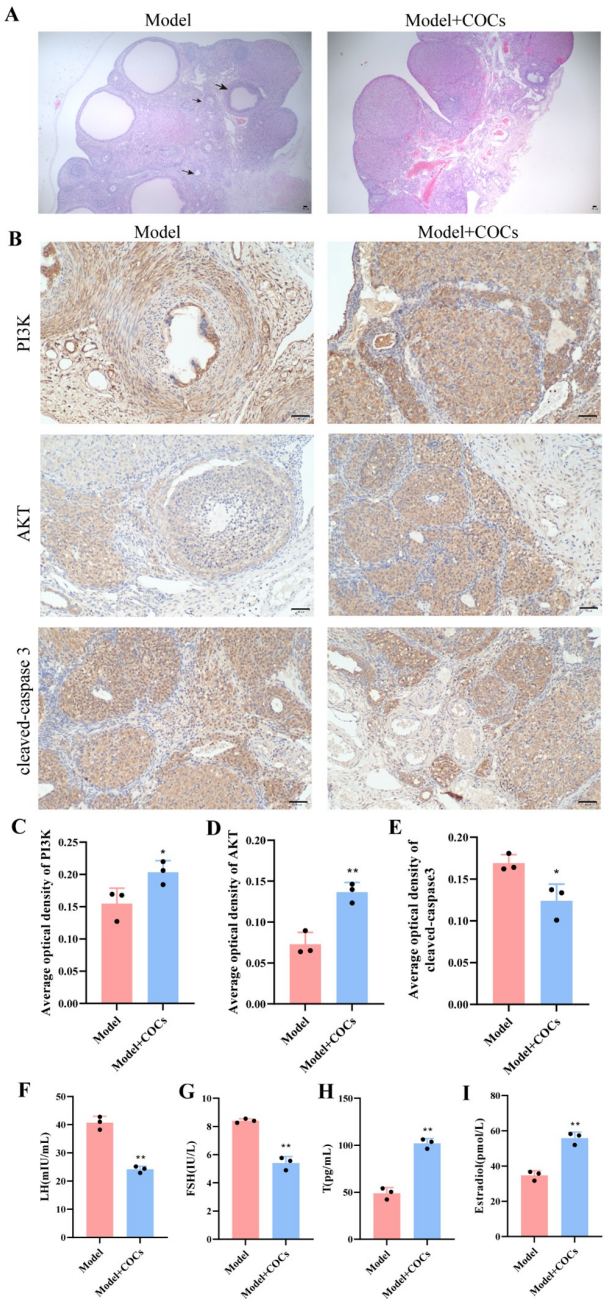

Fig. 1. Effects of COCs on ovarian structure, apoptosis, and hormonal levels in POI rats. (A) Hematoxylin-eosin staining of ovarian tissues in Model and Model + COCs groups; arrows indicate closed follicles in which granular cells are loosely arranged. Scale bar = 50 μm. (B–E) Immunohistochemical detection of expression levels of PI3K, AKT and cleaved-caspase 3 proteins. Scale bar = 50 μm. (F–I) Enzyme-linked immunosorbent assay (ELISA) determination of LH, FSH, T and estradiol levels in rat serum. Data are expressed as mean ± standard deviation (SD) of three independent experiments ($n = 3$); analyzed using *t*-test, * $p < 0.05$, ** $p < 0.01$. Abbreviations: COCs, combined oral contraceptives; FSH, follicle-stimulating hormone; LH, luteinizing hormone; POI, premature ovarian insufficiency; T, testosterone.

demonstrated a notable decrease in the expression level of the activated form of *Caspase 3* ($p < 0.05$), specifically the cleaved-caspase 3 protein ($p < 0.001$), in comparison to the Model group (Fig. 3F–T). The above outcomes show that COCs treatment significantly reduces POI-induced apoptosis of ovarian granulosa cells in rats, improves cell activity and estradiol secretion, and effectively inhibits apoptosis of ovarian granulosa cells in POI rats by enhancing PI3K/AKT signaling pathway, up-regulating Bcl-2 levels, and decreasing the expression of Bax and cleaved-caspase 3.

Effect of IL-11 on PI3K/AKT Signaling Pathway in Apoptosis of Rat Ovarian Granulosa Cells

Based on the aforementioned results, it can be seen that the Model group exhibited a marked reduction in IL-11 expression levels. Furthermore, research has indicated that IL-11 can influence the proliferation of ovarian granulosa cells in dairy cows [12]. To further explore whether IL-11 could regulate apoptosis of ovarian granulosa cells via the PI3K/AKT signaling pathway, we first overexpressed IL-11 in ovarian granulosa cells of POI rats. The findings revealed that, in comparison to the oe-NC group, the oe-IL-11 group exhibited a notable decrease in the apoptosis rate and a concurrent increase in cellular activity ($p < 0.001$) (Fig. 4A–C). Additionally, the oe-IL-11 group demonstrated a markedly elevated estradiol concentration compared to the oe-NC group in rats ($p < 0.05$) (Fig. 4D). qPCR analysis indicated that *IL-11* overexpression led to a marked upregulation of *Bcl-2* and *CYP19A1* mRNA levels ($p < 0.001$), accompanied by a downregulation of *Bax* ($p < 0.001$) and *Caspase 3* ($p < 0.01$) expression (Fig. 4E–K). Western blot analysis revealed a significant elevation in the ratios of p-PI3K/PI3K and p-AKT/AKT ($p < 0.001$) in the oe-IL-11 group, in contrast to the oe-NC group; additionally, overexpression of IL-11 also significantly decreased protein expression of cleaved-caspase 3, and protein expression patterns of IL-11, Bcl-2, Bax, and CYP19A1 aligned with the findings obtained from the qPCR analysis (Fig. 4L–S). The above results showed that the IL-11 overexpression significantly stimulated the PI3K/AKT signaling cascade, enhanced Bcl-2 expression, and diminished the levels of Bax and cleaved-caspase 3, ultimately leading to the suppression of ovarian granulosa cell apoptosis in rats with POI.

COCs Modulate Apoptosis in POI Rat Ovarian Granulosa Cells via IL-11/PI3K/AKT Signaling Pathway

The above findings indicate that overexpression of IL-11 inhibits granulosa cell apoptosis through activation of the PI3K/AKT pathway. In the same vein, we furthered the investigation by silencing IL-11 in POI rat granulosa cells and treating them with COCs. Flow cytometry analysis revealed that, compared with the sh-NC group, the sh-IL-11 group exhibited a significant increase in apoptosis rate, accompanied by marked decreases in cell viability

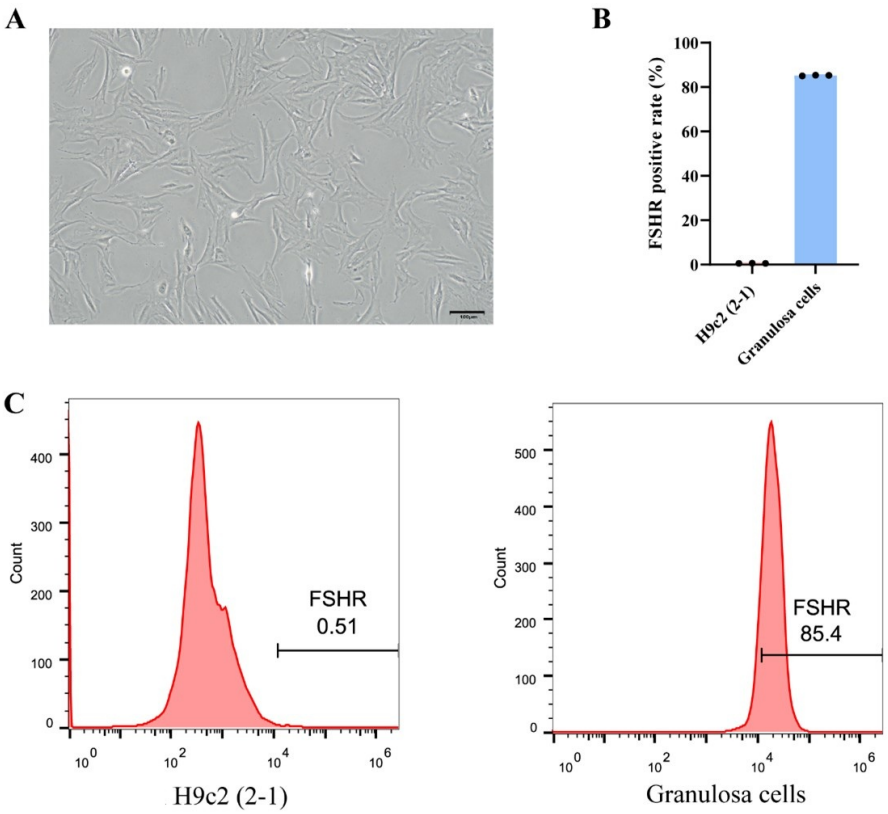

Fig. 2. Ovarian granulosa cells morphology and identification in POI rats. (A) Adherent growth status of POI rat ovarian granulosa cells after 24 h of culture. Scale bar = 100 μm. (B) Statistical analysis of follicle-stimulating hormone receptor (FSHR) positivity rate. Data are expressed as mean ± SD of three independent experiments ($n = 3$). (C) Detection of FSHR expression in H9c2 (2-1) and ovarian granulosa cells by flow cytometry.

and estradiol levels ($p < 0.001$); the apoptosis rate of sh-NC + COCs group was remarkably reduced ($p < 0.001$), while cell viability and estradiol levels were notably elevated ($p < 0.01$). Compared with the sh-IL-11, the combination of sh-IL-11 and COCs partially rescued the IL-11 silencing-induced elevation in apoptosis rate and reductions in cell viability and estradiol production (Fig. 5A–D). Further analysis using qPCR and Western blot revealed that, compared with the sh-NC group, IL-11 silencing significantly reduced IL-11 expression ($p < 0.001$). This downregulation of IL-11 led to decreased levels of Bcl-2 and CYP19A1 ($p < 0.001$), while promoting the expression of Bax ($p < 0.001$), *Caspase 3*, and cleaved-caspase 3 ($p < 0.001$). Concurrently, the ratios of p-PI3K/PI3K and p-AKT/AKT were significantly decreased ($p < 0.001$). In comparison to the sh-IL-11 group, the sh-IL-11 + COCs group showed notable increases in expression levels of IL-11, CYP19A1 ($p < 0.001$), and *Bcl-2* ($p < 0.05$). The expression levels of Bax, *Caspase 3*, and cleaved-caspase 3 were remarkably reduced in the sh-IL-11+COCs group ($p < 0.001$). Additionally, the ratios of p-PI3K/PI3K ($p < 0.01$) and p-AKT/AKT ($p < 0.05$) were significantly elevated in the sh-IL-11 + COCs group (Fig. 5E–S). Collectively, these findings demonstrated that IL-11 silencing was closely associated with a significant increase in granulosa cell apoptosis rate. The underlying mechanism may involve the suppression of the PI3K/AKT signaling pathway and the dysregulation of apoptosis-related proteins. COCs may upregulate the expression of IL-11, activate PI3K/AKT signaling pathway, restore the levels of anti-apoptotic proteins Bcl-2 and CYP19A1, and inhibit the expression of pro-apoptotic proteins Bax and members of the caspase family, thus improving the survival and function of granulosa cells in POI rats.

Discussion

POI—a disease with a huge pathological impact on female fertility—is treatable with COCs, although the mechanism of action remains largely obscure [26]. Experiments involving HE staining, immunohistochemistry, ELISA, qPCR, and Western blotting revealed that COCs could improve the pathology of ovarian tissue in POI rats and inhibit the apoptosis of ovarian granulosa cells through the IL-11/PI3K/AKT pathway.

A major clinical manifestation of POI is the premature decline of ovarian function, characterized by primordial follicular deficiency and abnormal follicular growth and de-

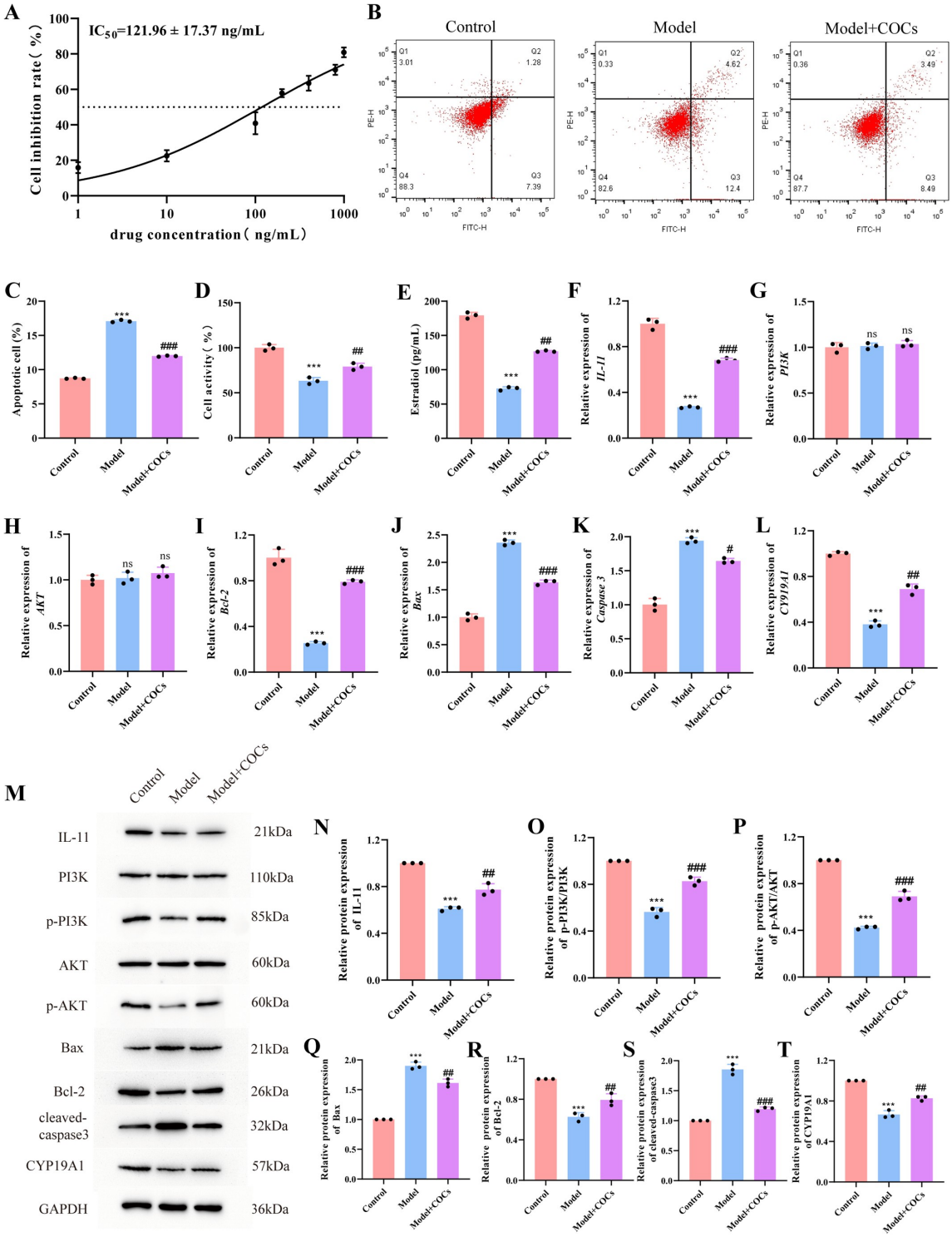

Fig. 3. Modulatory impact of COCs on apoptosis in ovarian granulosa cells of rats with POI. (A) Calculation of IC50. Data are expressed as mean ± SD of three independent experiments (n = 3). (B,C) Cell apoptosis detection in the control, Model and Model + COCs groups. (D) Cell counting kit-8 (CCK-8) assay for the detection of cellular activity. (E) Determination of estradiol levels in ovarian granulosa cells using ELISA. (F–L) qPCR detection of mRNA expression of *IL-11*, *PI3K*, *AKT*, *Bcl-2*, *Bax*, *Caspase 3*, *CYP19A1*. (M–T) Western blot detection of IL-11, PI3K, p-PI3K, AKT, p-AKT, Bax, Bcl-2, cleaved-caspase 3, CYP19A1 protein levels. Data are expressed as mean ± SD of three independent experiments (n = 3); analyzed using one-way ANOVA. Notes: ns, no significant difference ($p > 0.05$), $^{\#}$ $p < 0.05$, $^{\#\#}$ $p < 0.01$, ***,$^{\#\#\#}$ $p < 0.001$ compared with control and Model groups, respectively. Abbreviations: p-PI3K, phosphorylated phosphoinositide 3-kinase; p-AKT, phosphorylated protein kinase B; IC50, half-maximal inhibitory concentration; ANOVA, Analysis of variance.

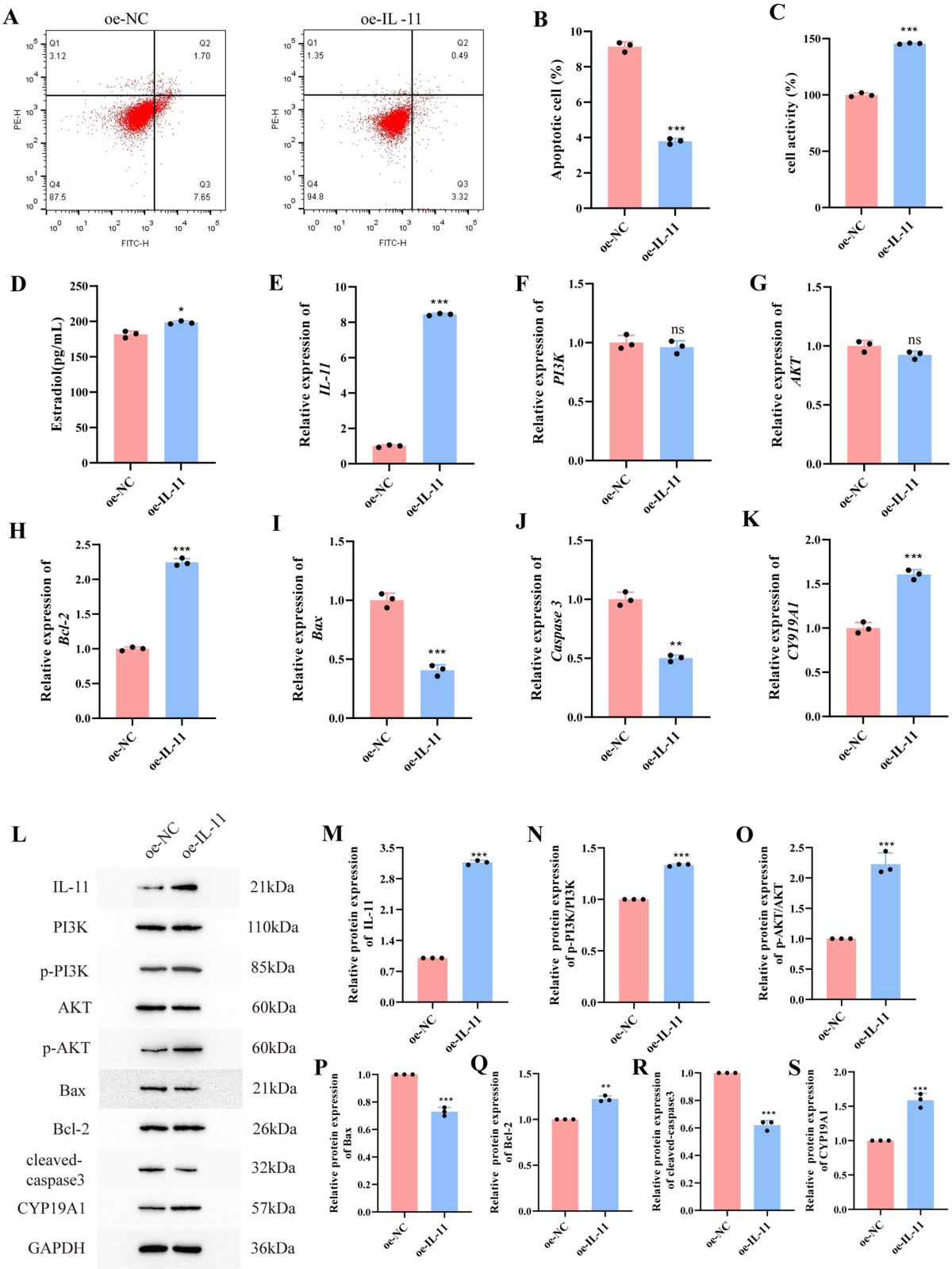

Fig. 4. Impact of overexpression of IL-11 on apoptosis of ovarian granulosa cells in POI rats. (A,B) Apoptosis detection in oe-NC and oe-IL-11 groups. (C) CCK-8 detection of cellular activity. (D) Determination of estradiol levels in ovarian granulosa cells using ELISA. (E–K) qPCR detection of mRNA expression of *IL-11, PI3K, AKT, Bcl-2, Bax*, *Caspase 3*, and *CYP19A1*. (L–S) Western blot detection of IL-11, PI3K, p-PI3K, AKT, p-AKT, Bax, Bcl-2, cleaved-caspase 3, and CYP19A1 protein levels. Data are expressed as mean ± SD of three independent experiments ($n = 3$); analyzed using *t*-test. Notes: ns, no significant difference, * $p < 0.05$, ** $p < 0.01$, *** $p < 0.001$.

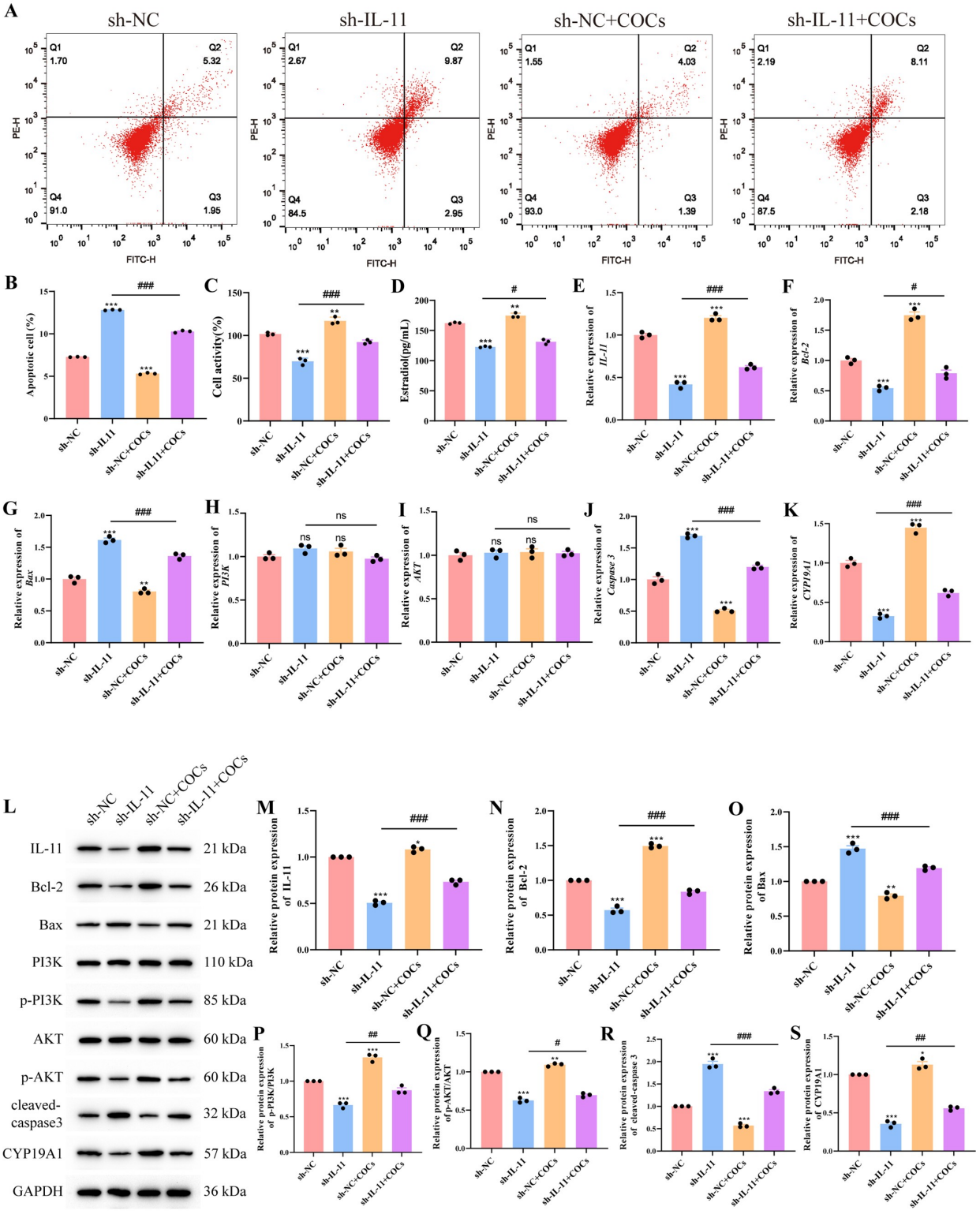

Fig. 5. COCs inhibit apoptosis of POI rat ovarian granulosa cells through IL-11/PI3K/AKT pathway. (A,B) Detection of apoptosis in the sh-NC, sh-IL-11, sh-NC + COCs and sh-IL-11 + COCs groups. (C) CCK-8 detection of cellular activity. (D) Determination of estradiol levels in ovarian granulosa cells using ELISA. (E–K) qPCR detection of mRNA expression of *IL-11*, *Bcl-2*, *Bax*, *PI3K*, *AKT*, *Caspase 3*, and *CYP19A1*. (L–S) Western blot detection of IL-11, Bcl-2, Bax, PI3K, p-PI3K, AKT, p-AKT, cleaved-caspase 3, and CYP19A1 protein levels. Data are expressed as mean ± SD of three independent experiments (n = 3); analyzed using one-way ANOVA. Notes: ns: no significant difference; *,# $p < 0.05$, **,## $p < 0.01$, ***,### $p < 0.001$ compared with sh-NC and sh-IL-11 groups, respectively.

velopment [27]. Since the granulosa cells play a pivotal role in the development and maturation of follicles [28], this study was designed to focus on the ovarian granulosa cells in POI rats and showed that COCs treatment could not only improve their status, but also significantly reduced LH and FSH levels and increased testosterone and estradiol levels in rat serum, consistent with findings reported by Cui and colleagues [29]. Activation of PI3K/AKT can promote apoptosis through cleaved-caspase, an activated form that acts on caspase 3 [30]. In the current study, we found that the expression of PI3K, AKT and cleaved-caspase 3 proteins in the Model + COCs group decreased notably in comparison with the Model group, suggesting that COCs might inhibit the apoptosis of ovarian granulosa cells in POI rats by activating the PI3K/AKT signaling pathway.

Bax and Bcl-2 are downstream effectors of the PI3K/AKT signaling pathway, and their ratio has an important indicative function for apoptosis. Research has shown that ethylene dithiocarbamate can induce apoptosis by increasing the expression of Bax [31]. Similarly, our study indicated that COCs treatment markedly decreased the level of Bax and increased the expression of Bcl2 in the ovaries of POI rats, thereby inhibiting the apoptosis of ovarian granulosa cells in rats. The *CYP19A1* gene encodes cytochrome P450 aromatase, which regulates the biosynthesis of estrogen [32]. In this study, we found that COCs treatment significantly raised the gene expression of *CYP19A1* and its serum level in the primary ovarian granulosa cells of POI rats. In addition, the treatment of COCs significantly increased the expression of IL-11, a multipotent cytokine that exerts a crucial inhibitory effect on apoptosis, in the ovarian granulosa cells of POI rats [33]. Meanwhile, COCs treatment remarkably enhanced the expression levels of p-PI3K/PI3K, p-AKT/AKT, and cleaved-caspase 3, thereby inhibiting the apoptosis of ovarian granulosa cells and improving cell activity. We speculate that the inhibited apoptosis of ovarian granulosa cells could be attributed to the action of COCs on the IL-11/PI3K/AKT pathway, a postulation inspired by research indicating that IL-11 activates the AKT pathway in NSCLC cells [34].

In this study, we further extended the experiments to IL-11 overexpression and gene interference in rat ovarian granulosa cells. Our experimental findings revealed that an IL-11 overexpression contributed to a marked reduction of apoptotic rate, increased cell activity, enhanced activity of the PI3K/AKT signaling pathway, and notably increased Bcl-2 levels, accompanied by suppressed expression of Bax and cleaved caspase 3. In alignment with our results, Moodley *et al*. [35] have demonstrated that elevated IL-11 expression led to a significant reduction in Bax and an increase in Bcl-2, consequently inhibiting apoptosis in pulmonary fibroblasts. On the other hand, interfering with the IL-11 led to the opposite results. This suggests a key role of IL-11 in the COCs treatment for the POI rats, potentially mediated through the activation of the PI3K/AKT signaling cascade and modulation of Bcl-2 and Bax expression levels, which eventually leads to the ovarian granulosa cell apoptosis through the Caspase 3 pathway. Finally, we explored whether COCs regulated the apoptosis of ovarian granulosa cells in POI rats via the IL-11/PI3K/AKT pathway. The results showed that COCs treatment markedly decreased the apoptotic rate in the sh-IL-11 + COCs group, enhanced cellular activity, and elevated estradiol levels. These findings further support the hypothesis that COCs modulate apoptosis in ovarian granulosa cells of POI rats via the IL-11/PI3K/AKT pathway.

In vitro activation is known as one of the effective methods for POI treatment by stimulating follicular development [36]. The PI3K/AKT pathway plays a crucial role in maintaining the quiescent state of primordial follicles, while PTEN serves as a negative regulator of this pathway [37]. The study has shown that Dingkun Pill can protect ovarian function by regulating PTEN expression in ovarian tissues of POI mice, which is closely associated with the inhibited activation of PI3K/AKT/FOXO3a signaling pathway [38]. The use of PI3K activators and PTEN inhibitors in human ovarian fragment cultures for *in vitro* activation of dormant follicles has been proposed as a treatment for infertility in POI patients [39], with two full-term births in POI patients receiving *in vitro* activation reported as successful cases [40]. It has been reported that IL-11 and IL-11Rα were highly expressed in ovarian tissues, and IL-11Rα knockdown promoted ovarian granulosa cell apoptosis [12]. This finding concurs with our findings that the IL-11/PI3K/AKT pathway plays a crucial role in the POI treatment using COCs to modulate the granulosa cell apoptosis, corroborating the IL-11/PI3K/AKT pathway as a novel therapeutic target for POI. Furthermore, the IL-11/PI3K/AKT pathway also exerts critical functions in other areas of reproductive health. For instance, the PI3K/AKT pathway is involved in endometrial epithelial cell proliferation, differentiation, and angiogenesis [41], while IL-11 modulates endometrial epithelial cell adhesion [42]. The proliferative imbalance of endometrial epithelial cells is closely linked to endometrial cancer development [43], suggesting that the IL-11/PI3K/AKT axis can serve as a pharmacological target for endometrial cancer treatment.

The current research established a theoretical groundwork for advancing the clinical application of COCs in POI treatment. However, due to significant physiological, genetic, and metabolic differences between humans and rats, further exploration is required before translating these findings into clinical practice. Furthermore, beyond the effects of COCs on ovarian granulosa cell apoptosis primarily investigated in this study, COCs have also been found to exert significant impacts on processes such as inflammation and oxidative stress [44,45]. These processes also play critical roles in regulating granulosa cell apoptosis; for instance, inflammatory responses and oxidative stress can independently influence ovarian granulosa cell apoptosis by acting

on the nuclear factor kappa B (NF-κB) signaling pathway and the Sirt3-Sod2 axis, respectively [46,47]. Therefore, future studies should explore the impact of COCs on inflammation, oxidative stress, and other related pathways to comprehensively elucidate their mechanistic roles in POI pathogenesis.

Conclusion

The current study showed that treatment using COCs could effectively ameliorate the pathological condition of ovarian granulosa cells in POI rats, reduce serum LH and FSH levels, and increase testosterone and estradiol levels, thereby inhibiting ovarian granulosa cell apoptosis through the COCs-induced activation of the IL-11/PI3K/AKT signaling pathway. Therefore, this study offers novel findings regarding the previously underexplored role of COCs involving modulation of the IL-11/PI3K/AKT signaling pathway, providing a new therapeutic target for the treatment of POI.

Availability of Data and Materials

The analyzed data sets generated during the study are available from the corresponding author on reasonable request.

Author Contributions

MLC: Data curation, Formal analysis, Methodology, Validation, Visualization, Writing-original draft, Funding acquisition, Writing-Critical revision. FZ: Data curation, Writing-Critical revision, Funding acquisition. FY and LZ: Data curation, Writing-Critical revision. LZe: Funding acquisition, Methodology, Project administration, Resources, Supervision, Writing-original draft, Writing-Critical revision. All authors have read and approved the final manuscript. All authors have participated sufficiently in the work and agreed to be accountable for all aspects of the work.

Ethics Approval and Consent to Participate

All animal experiments were conducted in accordance with the guidelines of the Institutional Animal Care and Use Committee (IACUC) and approved by the Ethics Committee of Guizhou University of Traditional Chinese Medicine (20230192).

Acknowledgment

Not applicable.

Funding

This study was supported by the Science and Technology Fund Project of Guizhou Provincial Health Commission (NO. gzwkj2022-408), Guizhou Provincial Graduate Student Research Fund Project (NO. YJSKYJJ [2021] 172), and Guizhou University of Traditional Chinese Medicine Intramural Subjects (NO. 3040-040200110).

Conflict of Interest

The authors declare no conflict of interest.

Supplementary Material

Supplementary material associated with this article can be found, in the online version, at https://doi.org/10.24976/Discov.Med.202537197.96.

References

[1] Torrealday S, Kodaman P, Pal L. Premature Ovarian Insufficiency - an update on recent advances in understanding and management. F1000Research. 2017; 6: 2069. https://doi.org/10.12688/f1000research.11948.1.

[2] McGlacken-Byrne SM, Conway GS. Premature ovarian insufficiency. Best Practice & Research. Clinical Obstetrics & Gynaecology. 2022; 81: 98–110. https://doi.org/10.1016/j.bpobgyn.2021.09.011.

[3] Regan SLP, Knight PG, Yovich JL, Leung Y, Arfuso F, Dharmarajan A. Granulosa Cell Apoptosis in the Ovarian Follicle-A Changing View. Frontiers in Endocrinology. 2018; 9: 61. https://doi.org/10.3389/fendo.2018.00061.

[4] Chon SJ, Umair Z, Yoon MS. Premature Ovarian Insufficiency: Past, Present, and Future. Frontiers in Cell and Developmental Biology. 2021; 9: 672890. https://doi.org/10.3389/fcell.2021.672890.

[5] Obeng E. Apoptosis (programmed cell death) and its signals - A review. Brazilian Journal of Biology. 2021; 81: 1133–1143. https://doi.org/10.1590/1519-6984.228437.

[6] Edlich F. BCL-2 proteins and apoptosis: Recent insights and unknowns. Biochemical and Biophysical Research Communications. 2018; 500: 26–34. https://doi.org/10.1016/j.bbrc.2017.06.190.

[7] Chi XX, Zhang T, Chu XL, Zhen JL, Zhang DJ. The regulatory effect of Genistein on granulosa cell in ovary of rat with PCOS through Bcl-2 and Bax signaling pathways. The Journal of Veterinary Medical Science. 2018; 80: 1348–1355. https://doi.org/10.1292/jvms.17-0001.

[8] Chen Y, Guan F, Wang P, Liu W, Zhang W, Sun H, *et al*. Copper exposure induces ovarian granulosa cell apoptosis by activating the caspase-dependent apoptosis signaling pathway and corresponding changes in microRNA patterns. Ecotoxicology and Environmental Safety. 2023; 264: 115414. https://doi.org/10.1016/j.ecoenv.2023.115414.

[9] Tummers B, Green DR. Caspase-8: regulating life and death. Immunological Reviews. 2017; 277: 76–89. https://doi.org/10.1111/imr.12541.

[10] Fung KY, Louis C, Metcalfe RD, Kosasih CC, Wicks IP, Griffin MDW, *et al*. Emerging roles for IL-11 in inflammatory diseases. Cytokine. 2022; 149: 155750. https://doi.org/10.1016/j.cyto.2021.155750.

[11] Zhang B, Zhang HX, Shi ST, Bai YL, Zhe X, Zhang SJ, *et al*. Interleukin-11 treatment protected against cerebral ischemia/reperfusion injury. Biomedicine & Pharmacotherapy. 2019; 115: 108816. https://doi.org/10.1016/j.biopha.2019.108816.

[12] Wu H, Sun P, Lv C, Zhao X, Liu M, Zhou Q, *et al*. Effects of IL-11/IL-11 Receptor Alpha on Proliferation and Steroidogenesis in Ovarian Granulosa Cells of Dairy Cows. Cells. 2023; 12: 673. https://doi.org/10.3390/cells12040673.

[13] Jang YJ, Park JI, Jeong SE, Seo YM, Dam PTM, Seo YW, *et al*. Regulation of interleukin-11 expression in ovulatory follicles of the rat ovary. Reproduction, Fertility, and Development. 2017; 29: 2437–2445. https://doi.org/10.1071/RD16460.

[14] Xu J, Li Y, Kang M, Chang C, Wei H, Zhang C, *et al*. Multiple forms of cell death: A focus on the PI3K/AKT pathway. Journal of Cellular Physiology. 2023; 238: 2026–2038. https://doi.org/10.1002/jcp.31087.

[15] Makker A, Goel MM, Mahdi AA. PI3K/PTEN/Akt and TSC/mTOR signaling pathways, ovarian dysfunction, and infertility: an update. Journal of Molecular Endocrinology. 2014; 53: R103–R118. https://doi.org/10.1530/JME-14-0220.

[16] Dong B, Zhu J, Chen X, Jiang H, Deng Y, Xu L, *et al*. The Emerging Role of Interleukin-(IL)-11/IL-11R in Bone Metabolism and Homeostasis: From Cytokine to Osteokine. Aging and Disease. 2023; 14: 2113–2126. https://doi.org/10.14336/AD.2023.0306.

[17] Zhuang Z, Pan X, Zhao K, Gao W, Liu J, Deng T, *et al*. The Effect of Interleukin-6 (IL-6), Interleukin-11 (IL-11), Signal Transducer and Activator of Transcription 3 (STAT3), and AKT Signaling on Adipocyte Proliferation in a Rat Model of Polycystic Ovary Syndrome. Medical Science Monitor: International Medical Journal of Experimental and Clinical Research. 2019; 25: 7218–7227. https://doi.org/10.12659/MSM.916385.

[18] Wang X, Che X, Liu C, Fan Y, Bai M, Hou K, *et al*. Cancer-associated fibroblasts-stimulated interleukin-11 promotes metastasis of gastric cancer cells mediated by upregulation of MUC1. Experimental Cell Research. 2018; 368: 184–193. https://doi.org/10.1016/j.yexcr.2018.04.028.

[19] Bhattacharya SM, Ghosh M, Basu R. Effects of ethinyl estradiol and desogestrel on clinical and metabolic parameters in Indian patients with polycystic ovary syndrome. The Journal of Obstetrics and Gynaecology Research. 2012; 38: 285–290. https://doi.org/10.1111/j.1447-0756.2011.01682.x.

[20] De Leo V, Di Sabatino A, Musacchio MC, Morgante G, Scolaro V, Cianci A, *et al*. Effect of oral contraceptives on markers of hyperandrogenism and SHBG in women with polycystic ovary syndrome. Contraception. 2010; 82: 276–280. https://doi.org/10.1016/j.contraception.2010.04.002.

[21] Cora MC, Kooistra L, Travlos G. Vaginal Cytology of the Laboratory Rat and Mouse: Review and Criteria for the Staging of the Estrous Cycle Using Stained Vaginal Smears. Toxicologic Pathology. 2015; 43: 776–793. https://doi.org/10.1177/0192623315570339.

[22] Webber L, Anderson RA, Davies M, Janse F, Vermeulen N. HRT for women with premature ovarian insufficiency: a comprehensive review. Human Reproduction Open. 2017; 2017: hox007. https://doi.org/10.1093/hropen/hox007.

[23] Nair AB, Jacob S. A simple practice guide for dose conversion between animals and human. Journal of Basic and Clinical Pharmacy. 2016; 7: 27–31. https://doi.org/10.4103/0976-0105.177703.

[24] Rio DC, Ares M, Jr, Hannon GJ, Nilsen TW. Purification of RNA using TRIzol (TRI reagent). Cold Spring Harbor Protocols. 2010; 2010: pdb.prot5439. https://doi.org/10.1101/pdb.prot5439.

[25] Panghiyangani R, Soeharso P, Andrijono, Suryandari DA, Wiweko B, Kurniati M, *et al*. CYP19A1 Gene Expression in Patients with Polycystic Ovarian Syndrome. Journal of Human Reproductive Sciences. 2020; 13: 100–103. https://doi.org/10.4103/jhrs.JHRS_142_18.

[26] Kirshenbaum M, Orvieto R. Premature ovarian insufficiency (POI) and autoimmunity-an update appraisal. Journal of Assisted Reproduction and Genetics. 2019; 36: 2207–2215. https://doi.org/10.1007/s10815-019-01572-0.

[27] Jiao X, Zhang H, Ke H, Zhang J, Cheng L, Liu Y, *et al*. Premature Ovarian Insufficiency: Phenotypic Characterization Within Different Etiologies. The Journal of Clinical Endocrinology and Metabolism. 2017; 102: 2281–2290. https://doi.org/10.1210/jc.2016-3960.

[28] Cavalcanti GS, Carvalho KC, Ferreira CDS, Alvarez PAC, Monteleone PAA, Baracat EC, *et al*. Granulosa cells and follicular development: a brief review. Revista Da Associacao Medica Brasileira (1992). 2023; 69: e20230175. https://doi.org/10.1590/1806-9282.20230175.

[29] Cui L, Bao H, Liu Z, Man X, Liu H, Hou Y, *et al*. hUMSCs regulate the differentiation of ovarian stromal cells via TGF-β_1/Smad3 signaling pathway to inhibit ovarian fibrosis to repair ovarian function in POI rats. Stem Cell Research & Therapy. 2020; 11: 386. https://doi.org/10.1186/s13287-020-01904-3.

[30] Li D, Ni S, Miao KS, Zhuang C. PI3K/Akt and caspase pathways mediate oxidative stress-induced chondrocyte apoptosis. Cell Stress & Chaperones. 2019; 24: 195–202. https://doi.org/10.1007/s12192-018-0956-4.

[31] Ali D, Tripathi A, Al Ali H, Shahi Y, Mishra KK, Alarifi S, *et al*. ROS-dependent Bax/Bcl2 and caspase 3 pathway-mediated apoptosis induced by zineb in human keratinocyte cells. OncoTargets and Therapy. 2018; 11: 489–497. https://doi.org/10.2147/OTT.S140358.

[32] El-Bayomi KM, Saleh AA, Awad A, El-Tarabany MS, El-Qaliouby HS, Afifi M, *et al*. Association of CYP19A1 gene polymorphisms with anoestrus in water buffaloes. Reproduction, Fertility, and Development. 2018; 30: 487–497. https://doi.org/10.1071/RD16528.

[33] Johnstone CN, Chand A, Putoczki TL, Ernst M. Emerging roles for IL-11 signaling in cancer development and progression: Focus on breast cancer. Cytokine & Growth Factor Reviews. 2015; 26: 489–498. https://doi.org/10.1016/j.cytogfr.2015.07.015.

[34] Zhao M, Liu Y, Liu R, Qi J, Hou Y, Chang J, *et al*. Upregulation of IL-11, an IL-6 Family Cytokine, Promotes Tumor Progression and Correlates with Poor Prognosis in Non-Small Cell Lung Cancer. Cellular Physiology and Biochemistry: International Journal of Experimental Cellular Physiology, Biochemistry, and Pharmacology. 2018; 45: 2213–2224. https://doi.org/10.1159/000488166.

[35] Moodley YP, Misso NLA, Scaffidi AK, Fogel-Petrovic M, McAnulty RJ, Laurent GJ, *et al*. Inverse effects of interleukin-6 on apoptosis of fibroblasts from pulmonary fibrosis and normal lungs. American Journal of Respiratory Cell and Molecular Biology. 2003; 29: 490–498. https://doi.org/10.1165/rcmb.2002-0262OC.

[36] Zhai J, Yao G, Dong F, Bu Z, Cheng Y, Sato Y, *et al*. In Vitro Activation of Follicles and Fresh Tissue Auto-transplantation in Primary Ovarian Insufficiency Patients. The Journal of Clinical Endocrinology and Metabolism. 2016; 101: 4405–4412. https://doi.org/10.1210/jc.2016-1589.

[37] Rosario R, Anderson RA. Novel approaches to fertility restoration in women with premature ovarian insufficiency. Climacteric: the Journal of the International Menopause Society. 2021; 24: 491–497. https://doi.org/10.1080/13697137.2020.1856806.

[38] Su C, Zhang R, Zhang X, Lv M, Liu X, Ao K, *et al*. Dingkun Pill modulate ovarian function in chemotherapy-induced premature ovarian insufficiency mice by regulating PTEN/PI3K/AKT/FOXO3a signaling pathway. Journal of Ethnopharmacology. 2023; 315: 116703. https://doi.org/10.1016/j.jep.2023.116703.

[39] Fàbregues F, Ferreri J, Méndez M, Calafell JM, Otero J, Farré R. *In Vitro* Follicular Activation and Stem Cell Therapy as a Novel

Treatment Strategies in Diminished Ovarian Reserve and Primary Ovarian Insufficiency. Frontiers in Endocrinology. 2021; 11: 617704. https://doi.org/10.3389/fendo.2020.617704.

[40] Suzuki N, Yoshioka N, Takae S, Sugishita Y, Tamura M, Hashimoto S, *et al*. Successful fertility preservation following ovarian tissue vitrification in patients with primary ovarian insufficiency. Human Reproduction. 2015; 30: 608–615. https://doi.org/10.1093/humrep/deu353.

[41] Gentilini D, Busacca M, Di Francesco S, Vignali M, Viganò P, Di Blasio AM. PI3K/Akt and ERK1/2 signalling pathways are involved in endometrial cell migration induced by 17beta-estradiol and growth factors. Molecular Human Reproduction. 2007; 13: 317–322. https://doi.org/10.1093/molehr/gam001.

[42] Marwood M, Visser K, Salamonsen LA, Dimitriadis E. Interleukin-11 and leukemia inhibitory factor regulate the adhesion of endometrial epithelial cells: implications in fertility regulation. Endocrinology. 2009; 150: 2915–2923. https://doi.org/10.1210/en.2008-1538.

[43] Chen J, Zhao KN, Li R, Shao R, Chen C. Activation of PI3K/Akt/mTOR pathway and dual inhibitors of PI3K and mTOR in endometrial cancer. Current Medicinal Chemistry. 2014; 21: 3070–3080. https://doi.org/10.2174/0929867321666140414095605.

[44] Cauci S, Xodo S, Buligan C, Colaninno C, Barbina M, Barbina G, *et al*. Oxidative Stress Is Increased in Combined Oral Contraceptives Users and Is Positively Associated with High-Sensitivity C-Reactive Protein. Molecules. 2021; 26: 1070. https://doi.org/10.3390/molecules26041070.

[45] Maia HJ, Casoy J. Non-contraceptive health benefits of oral contraceptives. The European Journal of Contraception & Reproductive Health Care: the Official Journal of the European Society of Contraception. 2008; 13: 17–24. https://doi.org/10.1080/13625180701712745.

[46] Wang J, Wu J, Zhang Y, Zhang J, Xu W, Wu C, *et al*. Growth hormone protects against ovarian granulosa cell apoptosis: Alleviation oxidative stress and enhancement mitochondrial function. Reproductive Biology. 2021; 21: 100504. https://doi.org/10.1016/j.repbio.2021.100504.

[47] Xue H, Hu Z, Liu S, Zhang S, Yang W, Li J, *et al*. The mechanism of NF-κB-TERT feedback regulation of granulosa cell apoptosis in PCOS rats. PLoS ONE. 2024; 19: e0312115. https://doi.org/10.1371/journal.pone.0312115.